Veterinary Microbiology 237 (2019) 108407

Contents lists available at ScienceDirect

Veterinary Microbiology

journal homepage: www.elsevier.com/locate/vetmic

gga-miR-21 modulates *Mycoplasma gallisepticum* (HS strain)-Induced inflammation via targeting MAP3K1 and activating MAPKs and NF-κB pathways

Yabo Zhao, Mengyun Zou, Yingfei Sun, Kang Zhang, Xiuli Peng*

Key Laboratory of Agricultural Animal Genetics, Breeding and Reproduction (Huazhong Agricultural University), Ministry of Education, College of Animal Science and Technology and College of Veterinary Medicine, Huazhong Agricultural University, Wuhan, 430070, China

ARTICLE INFO

Keywords:
gga-miR-21
MAP3K1
Mycoplasma gallisepticum (HS strain)
Inflammatory cytokines
NF-κB signaling pathway

ABSTRACT

Mycoplasma gallisepticum (MG) can target host cells and cause chronic respiratory disease (CRD) in chickens that is characterized by pMGA and concomitant. Although microRNAs (miRNAs) have been manifested are crucial regulatory noncoding RNAs with important effects on microbial pathogenesis and inflammatory response, how miRNAs regulate MG-induced inflammation remains to be discovered. The results showed that gga-miR-21 was up-regulated in MG-infected chicken embryonic lungs and MG infection of chicken embryo fibroblast cells (DF-1) compared with the control group. Overexpression of gga-miR-21 increased the inflammatory cytokines production, including tumor necrosis factor alpha (TNF-α), interleukin-1β (IL-1β), interleukin-6 (IL-6), and interleukin-8 (IL-8) after MG infection, knockdown of gga-miR-21 had thoroughly inverse effects. Gene expression data combined with bioinformatics analysis and luciferase reporter assays demonstrated that mitogen-activated protein kinase kinase kinase 1(*MAP3K1*) was a novel target of gga-miR-21. The inhibition of *MAP3K1* by gga-miR-21 resulted in the accumulation of NF-κB in the nucleus, which in turn generate higher inflammatory cytokines. Furthermore, upregulation of gga-miR-21 significantly inhibited MG propagation and promoted MG-infected DF-1 cells proliferation by increasing the cell cycle progression and suppressing cell apoptosis. Our study provides evidence for proinflammatory effects of gga-miR-21 which is mediated at least in part by targeting MAP3K1 in the MG-infected DF-1 cells. gga-miR-21 activates MAPKs and NF-κB signaling pathways via targeting *MAP3K1*, and then promotes the production of inflammatory cytokines and cell proliferation by increasing the cell cycle progression and suppressing cell apoptosis to defend against MG infection.

1. Introduction

Inflammatory responses play decisive roles in host defense against microbial pathogen infections (Ferreromiliani et al., 2007). Without inflammation, wounds and infections cannot heal. However, Excessive inflammation also causes tissue damages and host diseases (Kim et al., 2014). MG is the causative agent of chronic respiratory disease, an epidemic disease of poultry, which causes serious inflammation in lungs and tracheas of chickens and turkeys around the world (Cookson and Shivaprasad, 1994). MG infections cause considerable economic losses to the poultry industry as a result of reduced egg production, decreased weight gain and increased embryo mortality (Bi and Xu, 1997). It was reported that HeLa cells and chicken fibroblast cells can be directly infected by MG and act as a reservoir for MG (Winner et al., 2000). During infection, MG targets host cells by the adhesin proteins and results in the activation of the nuclear factor-kappaB (NF-κB) signaling and the production of several inflammatory cytokines, for instance, interleukin-1β (IL-1β), interleukin-6 (IL-6), interleukin-8 (IL-8) and tumor necrosis factor alpha (TNF-α) (Hu et al., 2016b). As a pivotal transcriptional factor, NF-κB controls the expression of genes involved in intrinsic and adaptive immunity, and cell proliferation, differentiation, and apoptosis, especially inflammatory reaction and the rapid response to pathogenic microorganism infection. Increasing evidence indicates that the active involvement of the NF-κB signaling cascade generally leads to the production of chemokines and pro-inflammatory cytokines (Hayden and Ghosh, 2008).The production of various pro-inflammatory mediators can play a protective role or originate an inconvertible immune response resulting in necroptosis. Nevertheless, the regulation of MG-induced lung inflammation processes is not well documented. MG-HS strain is a virulent strain with markedly different pathogenicity, The adhesin protein pMGA1.2, the crucial adhesin on the surface of MG-HS strain, is responsible for MG-HS to propagate in

* Corresponding author.
E-mail address: xlpengsishun@mail.hzau.edu.cn (X. Peng).

https://doi.org/10.1016/j.vetmic.2019.108407
Received 30 May 2019; Received in revised form 7 August 2019; Accepted 3 September 2019

Table 1
Sequences of DNA primers.

Name	Primer sequences (5′-3′)	Accession No.
Primers for 3′-UTR Cloning		
MAP3K1 3′-UTR-F	GCCCTCGAGTAAGGCAGGTTTT	XM_015277577.1
MAP3K1 3′-UTR-R	ATAGCGGCCGCAACCAATGACACT	
Mut-P-M 3′-UTR-F	CAGGATAAACTAAAGCCGCTACAGTACATTTAAAAATGTACAATACGGATTGG	XM_015277577.1
Mut-P-M 3′-UTR-R	AATGTACTGTAGCGGCTTTAGTTTATCCTGAGTCTTTGAGAAATAACCAATTC	
Primers for RT-qPCR		
GAPDH-F	GAGGGTAGTGAAGGCTGCTG	NM-204305
GAPDH-R	CACAACACGGTTGCTGTATC	
RT-gga-miR-21	CTCAACTGGTGTCGTGGAGTCGGCAATTCAGTTGAGTCAACATC	MIMAT0003774
gga-miR-21-F	CTGGTAGGTAGCTTATCAGACTG	MIMAT0003774
gga-miR-21-R	ACTGGTGTCGTGGAGTCGGC	
gga-5s-rRNA-F	CCATACCACCCTGGAAACGC	
gga-5s-rRNA-R	TACTAACCGAGCCCGACCCT	
MAP3K1-F	CCTGAGGAAACAAGTCGTCG	XM_015277577.1
MAP3K1-R	TGGAACACTCGCAGCATA	
pMGA1.2-F	TGAAACTTCGCTCAAAGAG	AF275312
pMGA1.2-R	TGTAACCCAACATCATCGT	
pre-miR-21-F	TCAGACTGATGTTGACTGTTGG	NR_031583.1
pre-miR-21-R	GAGATACCAAAATGTCAGACAGC	
pri-miR-21-F	TCCTGCCTGAATGTCCTCC	NR_031583.1
pri-miR-21-R	GCCTACCGACTGTTGTTGC	

animal tissues through binding to apolipoprotein A–I (ApoA–I) on host cells (Hu et al., 2016a).

Micro-ribonucleic acids (miRNAs) act as fine-tuners of gene expression that utilize sequence complementarity to bind to the 3′ UTR of the target mRNAs and decrease the stability or translation efficiency of target genes, they participate in the complex signaling network underlying various physiological and pathological processes, including cellular proliferation and differentiation, apoptosis, tumorigenesis and microbial infection (Ambros, 2004). Recently, these small RNAs have been found to contribute to the development and control of inflammatory responses in immune cells as well as non-immune cells (Bazzoni et al., 2009). For example, TLR4- triggered activation of NF-κB induces a negative feedback by increasing the expression of miR-146, which ultimately suppress TLR-induced signaling pathway and pro-inflammatory cytokines expression (Taganov et al., 2006). Critical roles for miR-181 in astrocyte-mediated inflammation have also been described (Hutchison et al., 2013). Moreover, we have reported the role of gga-miR-19a in regulating MG-mediated inflammatory cytokine production in both the DF-1 cells and the lungs of chicken embryos (Hu et al., 2016b). gga-miR-101 modulates MG–induced inflammation by targeting enhancer of zeste homolog 2 (EZH2) (Chen et al., 2015). Therefore, the functional study of miRNAs is conducive to uncover the intricate molecular pathways involved in microbial pathogenesis and inflammatory responses, and provide a theoretical basis for miRNA-mediated gene therapy.

miR-21 is highly conserved among mammalian species and plays diverse roles in different tissues and cell types (Sheedy, 2015). In allergic airway inflammation, miR-21 is up-regulated and modulates interleukin-12 (IL-12) by targeting IL-12p35 (Lu et al., 2009). In primary rat hepatocytes, miR-21 down-regulated the expression of PDCD4 to suppress cell apoptosis (Rodrigues et al., 2016). miR-21 was also reported to be involved in virus replication and NF-κB signaling at multiple levels (Sheedy, 2015). Our preliminary deep sequencing data revealed that many host miRNAs were differentially expressed, and gga-miR-21 was significantly up-regulated in the MG-infected embryonic lungs (Zhao et al., 2017), which suggests that it might play an important role in the response to the MG infection of chicken. In the present study, we verified that gga-miR-21 is up-regulated following MG infection. It is demonstrated that MG-mediated induction of gga-miR-21 increases NF-κB expression by direct suppression of *MAP3K1*, resulting in the aggravation of MG-induced production of inflammatory mediators. Further investigations revealed that gga-miR-21 restrains MG propagation and promotes the MG-infected DF-1 cell proliferation by promoting the cell cycle progression and inducing cell apoptosis. To the best of our knowledge, this is the first study to elucidate the role of gga-miR-21 as a regulator of MG-induced inflammation through the targeting of *MAP3K1*. This study indicated that gga-miR-21 may become a promising therapeutic target for the treatment of *Mycoplasmosis*.

2. Materials and methods

2.1. Reagents

Antibody against MEKK1 was acquired from Lifespan. Antibodies against p65, glyceraldehyde-3-phosphate dehydrogenase (GAPDH), and β-actin were purchased from Bio-swamp. Horseradish peroxidase-conjugated anti-mouse/rabbit secondary antibodies were from Sangon Biotech. The oligonucleotides of gga-miR-21 mimics (double-stranded RNA oligonucleotides, denoted as gga-miR-21) and gga-miR-21 inhibitor (single-stranded chemically modified oligonucleotides, denoted as miR-21-Inh) were synthesized from GenePharma. A random miRNA mimics that had not been found to suppress any chicken target genes (denoted as miR-21-NC), and a random miRNA inhibitor that had not been found to promote any chicken target genes (denoted as miR-21-Inh-NC) were also designed and synthesized to serve as the negative controls. Small interfering RNA (siRNA) oligonucleotide and control for MAP3K1 were purchased from RIBOBIO (denoted as si-MAP3K1 and NC). The sequences of all the primers used in this study are listed in Table 1. The sequences of RNA oligonucleotides are shown in Table 2.

2.2. Cell culture and treatment

DF-1 cells (chicken embryonic fibroblast cell line) were obtained

Table 2
Sequences of RNA oligonucleotides.

Name	Sequences (5′-3′)
gga-miR-21 mimics	UAGCAGCACGUAAAUAUUGGUG CCAAUAUUUACGUGCUGCUAUU
gga-miR-21 NC	UUCUCCGAACGUGUCACGUTT ACGUGACACGUUCGGAGAATT
gga-miR-21 inhibitor	CACCAAUAUUUACGUGCUGCUA
gga-miR-21 inhibitor NC	CAGUACUUUUGUGUAGUACAA
si-MAP3K1	CCCTGTGGATTCTTCTGTT

and authenticated from American Type Culture Collection (Rockville, MD, USA). Cells were maintained in Dulbecco's modified eagle medium (DMEM, Invitrogen, Carlsbad, CA, USA), supplemented with 10% fetal bovine serum (FBS, Invitrogen, USA) and 1% penicillin-streptavidin-glutamine (PSG, Invitrogen, USA). Cells were incubated at 39 °C in a 5% CO_2 humidified atmosphere. For transient transfection, DF-1 cells were plated evenly in 6-, 24- or 96-well plates and grown to 60% confluency without antibiotics and subsequently transfected with RNAs and/or plasmids using Lipofectamine 3000 (Invitrogen, USA). After 48 h, the cells in different groups were collected for further use. For MG-HS infection experiments, at 24 h post-transfection, cells were infected with MG-HS at the log phase (1×10^{10} CCU/ml) for the times mentioned in the figure legends.

2.3. Mycoplasma strains

MG-HS, a virulent strain, was conserved and donated by the State Key Laboratory of Agricultural Microbiology, Huazhong Agricultural University (Wuhan, China). It was isolated from a chicken farm in Hubei province of China (Bi and Ji, 1988; Bi and Xu, 1997). As previously methods, the MG-HS strain culture and concentration determination were conducted (Bi and Ji, 1988), and its viable number in suspension was measured using a color-changing unit (CCU) assay (Bi and Xu, 1997).

2.4. Infection experiments

One hundred embryos of White Leghorn specific-pathogen-free (SPF) chickens were incubated on the 9th day and the allantoic cavities were injected with 300 μl of MG-HS at 10^{10} CCU/ml. Other 100 chicken embryos were injected with the same dosage of the diluent to serve as controls. The viability of the chicken embryos was visually detected under a candling machine and the dead embryos were eliminated. The mortality rates of the chicken embryos of the infection and control groups were 12.3% and 7%, respectively. On germfree conditions, whole-lung tissue samples from six infected live chicken embryos and six controls were collected on days 5, 9, 10, and 11 post-infection and stored in RNA fixer (BioTeke Co., Ltd., Beijing, China). The experiment of DF-1 cells was infected with MG, DF-1 cells were plated in six-well plates without antibiotics. There were an experimental group and a control group when the cells in the experimental group reached 80–90% confluence, the experimental group was infected with 130 μl of MG at the mid-exponential phase (1×10^{10} CCU/ml). After 48 h infection, the cells in both groups were collected using RIPA buffer (Beyotime, China) or Trizol (Invitrogen, Carlsbad, CA, USA) for further experiments. Each infection experiment was repeated for three independent times with three triplicates of each sample.

2.5. Constructs and plasmids

The psi−CHECK™-2 dual-luciferase reporter vector (Promega, Madison, WI, USA) harboring the wild-type and mutant MAP3K1 3′-UTR, which were inserted into the *Xho I* and *Not I* restriction sites 3′ to the end of the *Renilla* gene, were used to check the effect of gga-miR-21 on *Renilla* activity. The full length of the wild-type MAP3K1 3′-UTR or fragments covering the putative gga-miR-21-binding site were amplified by RT-PCR following cDNA extraction from the lung tissues of chicken. The psi−CHECK™-2 mutant MAP3K1 3′-UTR construct was generated by inducing a point mutation using the overlap extension PCR method. The recombinant wild-type and mutant plasmids were named Luc-WT-MAP3K1 and Luc-Mut-MAP3K1, respectively. MAP3K1 CDS were amplified and cloned into the pcDNA3.1(+) vector (Invitrogen). The primers are listed in Table 1. All constructs were verified by sequencing.

2.6. Dual-luciferase reporter assay

DF-1 cells were seeded on 24-well plates at a density of 3×10^5 cells per well and cultured until the cells reached approximately 60% confluence. Cells were then transfected with 200 ng of the luciferase reporter plasmid and 10 pmol of gga-miR-21, miR-21-NC, miR-21-Inh or miR-21-Inh-NC using Lipofectamine 3000 (Invitrogen, USA). At 48 h post-transfection, the cells were collected, the Firefly and *Renilla* luciferase activities were determined using EnSpire & Multimode Reader (PerkinElmer, Inc., Waltham, USA) according to the manufacturer's protocol (Promega, USA). Three independent repeats were performed for all above transfection experiments.

2.7. Real-time quantitative PCR

According to the manufacturer's instructions, total RNA was extracted from tissues and cells using the TRIzol reagent (Invitrogen, Carlsbad, CA, USA), 1 μg RNA from each sample was used to synthesize cDNA using the Prime Script™ RT reagent kit with gDNA Eraser (TaKaRa, Japan). The real-time PCR was performed with TransStart Top Green qPCR SuperMix (TRANSGEN, China) on a CFX96 or CFX384 TouchTM instrument (Bio-Rad, USA). The expression levels of gga-miR-21, MAP3K1 and pMGA1.2 were measured by RT-qPCR. Chicken 5S-RNA and GAPDH mRNA were used as internal controls, respectively. The relative mRNA levels were calculated using the $2^{-\Delta\Delta Ct}$ method (Livak and Schmittgen, 2001). The data were analyzed using 7500 software v.2.0.1 (Applied Biosystems) with the automatic Ct settings for adapting the baselines and thresholds for Ct determination. The experiment was repeated three times, and the primers are listed in Table 1.

2.8. Immunofluorescence

After transfection for 48 h, DF-1 cells were fixed with 4% paraformaldehyde for 15 min and then washed three times with PBS for 5 min. Next, the cells were permeabilized by added 0.5% Triton X-100 (Sigma, USA) for 10 min and 1% bovine serum albumin (BSA) to incubate the cells for 45 min and block interactions with nonspecific proteins. Subsequently, the cells were incubated with specific antibodies against p65 overnight at 4 °C. The next day, the cells were washed three times with PBS for 10 min and then added with the goat anti-rabbit Alexa Fluor 594–labeled secondary antibody and incubated at room temperature for 2 h. Finally, the cell nuclei and p65 protein were immobilized and detected using mounting media containing DAPI. Images were viewed and obtained with Confocal Laser Scanning Microscope (ZEISS LSM 800 META, Carl Zeiss Imaging, Germany).

2.9. Electrophoretic immunosorbent assay (ELISA)

DF-1 cells in 6-well plates were transfected with gga-miR-21, miR-21-NC, miR-21-Inh or miR-21-Inh-NC and were incubated for 24 h and then either left uninfected or infected with 130 μl of MG-HS. The culture supernatants were drawn from the treated cells at 36 h post-infection, the protein levels of the culture supernatants were determined by TNF-α, IL-1β, IL6, and IL-8 enzyme-linked immunosorbent assay (ELISA) kits (Bio-Swamp, China) according to the manufacturer's instructions.

2.10. Western blotting assay

The total proteins were prepared using cell lysis buffer at 48 h post-transfection or post-infection. Protein concentrations were measured with a BCA Protein Assay Kit (TRANSGEN, China). And equal amounts of protein (10 μg) were separated by 12% SDS-polyacrylamide gel electrophoresis (SDS-PAGE) and transferred to nitrocellulose membranes (Beyotime, China) using a Mini Trans-Blot Cell (Bio-Rad, USA).

The membranes were blocked in 5% (w/v) non-fat milk for 1 h at room temperature and then incubated with the primary antibodies, including rabbit polyclonal anti-MEKK1, *β*-actin, or *GAPDH* overnight at 4℃. The membranes were then washed with TBST and incubated with goat anti-rabbit secondary antibody for 1.5 h at 37 ˚C. After washing with TBST, the protein binds on the membranes were visualized using an ECL™detection system (Bio-Rad, USA).

2.11. Cell proliferation, cell cycle and cell apoptosis

Cell proliferation was determined using real-time cell analyzer system (RTCA). Background measurements were taken from the wells by adding 50 μl of the same culture medium to the E-16 plates. And then the plates were calibrated using RTCA Software Package 1.2. DF-1 cells were plated at a density of 8×10^3 cells per well with fresh medium to a final volume of 200 μl and allowed to grow for 6 h at 39 ˚C with 5% CO_2 in the RTCA cradle. Subsequently, gga-miR-21, miR-21-NC, miR-21-Inh or miR-21-Inh-NC was transfected into DF-1 cells, respectively. At 24 h post-transfection, DF-1 cells were infected with 8 μl of MG-HS strain at 10^{10} CCU/ml. The impedance signals were recorded every 5 min up to 72 h.

The cell cycle and cell apoptosis assay were performed in 6-well plates. The indicated RNA oligonucleotides were transfected into DF-1 cells. At 24 h post-transfection, the cells were infected with 130 μl of MG-HS strain at 10^{10} CCU/ml. At 24 h post-infection, the percentages of the cells in the G1, S and G2 phases was analyzed with a flow cytometer, using to the cell cycle detection kit (DOJINDO, Shanghai, China). The cell apoptosis was measured with a flow cytometer, according to the manufacturer's protocol of the Annexin V-FITC Apoptosis Detection Kit (DOJINDO, Shanghai, China). And data was processed using the FlowJo7.6 software.

2.12. Statistical analysis

All experiments were performed three times with similar results, results are shown as the mean values ± SEM. SPSS software (SPSS 20.0, IBM, Armonk, NY, USA) was used for statistical analyses. One-way ANOVA or Student's *t*-test was determined for p-value calculations and p-value < 0.05 was considered to be statistically significant (* $P < 0.05$, ** $P < 0.01$, Different capital letters represent $P < 0.05$, Different lowercase letters represent $P < 0.01$).

3. Results

3.1. Upregulation of gga-miR-21 upon MG infection

Chicken embryos were infected with MG-HS on the 9th day of incubation. On the 5, 9, 10, and 11th days post-infection (the 14, 18, 19, and 20th days of egg hatching), gga-miR-21 displayed the large increase in its expression in the lungs of MG-infected chicken embryos (Fig. 1A). Similar to the results for mature gga-miR-21, primary gga-miR-21 transcripts (pri-miR-21) and gga-miR-21 precursors (pre-miR-21) were also investigated to be elevated in the MG-infected DF-1 cells (Fig. 1B, C, and D). These results demonstrate that gga-miR-21 expression is up-regulated after MG infection.

3.2. gga-miR-21 induces MG–mediated inflammatory cytokine production

Infection of cells with MG-HS results in immune response along with the production of other inflammatory cytokines. To identify whether gga-miR-21 regulates MG-mediated immune responses in DF-1 cells, we explored the role of gga-miR-21 in inflammatory cytokine production following MG infection. First, we detected the quality of synthetic gga-miR-21 mimics and inhibitor on the expression pattern of gga-miR-21. DF-1 cells were transfected with a gga-miR-21 mimics (denoted as gga-miR-21), a random miRNA mimics (denoted as miR-21-NC), a gga-miR-21 inhibitor (denoted as miR-21-Inh) or a random miRNA inhibitor (denoted as miR-21-Inh-NC), respectively. As expected, gga-miR-21 mimics increased gga-miR-21 levels markedly in DF-1 cells, whereas gga-miR-21 inhibitor diminished its levels **(**Fig. 2A**)**. DF-1 cells were transfected with gga-miR-21, miR-21-NC, miR-21-Inh or miR-21-Inh-NC for 24 h and then infected with 130 μl of MG-HS strain at 10^{10} CCU/ml [denoted as gga-miR-21(MG +), miR-21-NC(MG +), miR-21-Inh (MG +) or miR-21-Inh-NC (MG +), respectively] for 36 h. Enzyme-linked immunosorbent assay (ELISA) revealed that gga-miR-21 mimics significantly up-regulated the protein levels of TNF-α, IL-1β, IL6, and IL8 in the MG-infected DF-1 cells **(**Fig. 2B**)**. In contrast, the inhibition of endogenous gga-miR-21 significantly decreased the protein levels of TNF-α, IL-1β, IL6, and IL8 **(**Fig. 2C**)**. Thus, these data strongly indicate that gga-miR-21 induces the production of inflammatory cytokines in MG-infected cells.

3.3. gga-miR-21 targets MAP3K1

To understand the mechanism by which gga-miR-21 regulates inflammation, the specific target of gga-miR-21 was investigated further. By using several public miRNA target-prediction algorithms (miRBase, miRDB, TargetScan, RNAhybrid, and miRecords), *MAP3K1*, an important negative regulator of MAPKs and NF-κB signaling pathway, displayed potential seed matches for gga-miR-21. The sequence of target site in the 3′-UTR of *MAP3K1* is shown to be highly conserved among different species **(**Fig. 3A**)**. RNAhybrid was used to analyze the duplex and minimum free energy (mfe) between gga-miR-21 and the *MAP3K1* 3′-UTR. The mfe of the RNA duplex (-15.6 kCal/mol) indicated high stability **(**Fig. 3B**)**.

To confirm the possibility that *MAP3K1* can be repressed post-transcriptionally by gga-miR-21, we constructed dual-luciferase reporter plasmids carrying the *MAP3K1* 3′-UTR with the wild-type or mutant gga-miR-21 binding region to generate Luc-WT-MAP3K1 (3′-UTR) and Luc-Mut-MAP3K1 (3′-UTR) **(**Fig. 3C**)**. A marked reduction in luciferase levels was found in DF-1 cells co-transfected with gga-miR-21 mimic and wild-type *MAP3K1* (3′-UTR) luciferase reporter plasmid after 48 h, whereas mutation of 3 base pair in the gga-miR-21 target sequence led to a complete abrogation of the negative effect of gga-miR-21 on the expression of *MAP3K1* (3′-UTR) reporter constructs, blank means mock transfection **(**Fig. 3D**)**. These results indicate that the nucleotide sequence in the 3′-UTR of *MAP3K1* is a potential gga-miR-21 targeting site. To further validate *MAP3K1* as a target of gga-miR-21, the expression of endogenous *MAP3K1* was examined in DF-1 cells treated with gga-miR-21 mimics or inhibitor, blank means mock transfection. As expected, the over-expression of gga-miR-21 significantly suppressed *MAP3K1* mRNA and protein (MEKK1) levels **(**Fig. 3E**)**, whereas the suppression of *MAP3K1* could be restored in the presence of miR-21-Inh **(**Fig. 3F**)**, suggesting that *MAP3K1* expression could be inhibited by gga-miR-21 via both mRNA decay and translational repression. Taken together, these data suggest that *MAP3K1* is a direct target of gga-miR-21 and its expression is negatively regulated by gga-miR-21.

3.4. MAP3K1 expression is down-regulated in MG infection

To study the effect of MG infection on *MAP3K1*, we performed the infection experiments in *vitro* and in *vivo*. Chicken embryos were infected with MG-HS on the 9th hatching day. On the 5, 9, 10, and 11th days post-infection (the 14, 18, 19, and 20th days of egg hatching), RT-qPCR showed that the *MAP3K1* expression levels were significantly lower in the lungs of the MG-infected chicken embryos compared with the control **(**Fig. 4A**)**. As expected, the mRNA and protein levels of MAP3K1 were both significantly decreased in MG-infected DF-1 cells after 48 h detected by RT-qPCR and western blot analysis separately **(**Fig. 4B**)**.

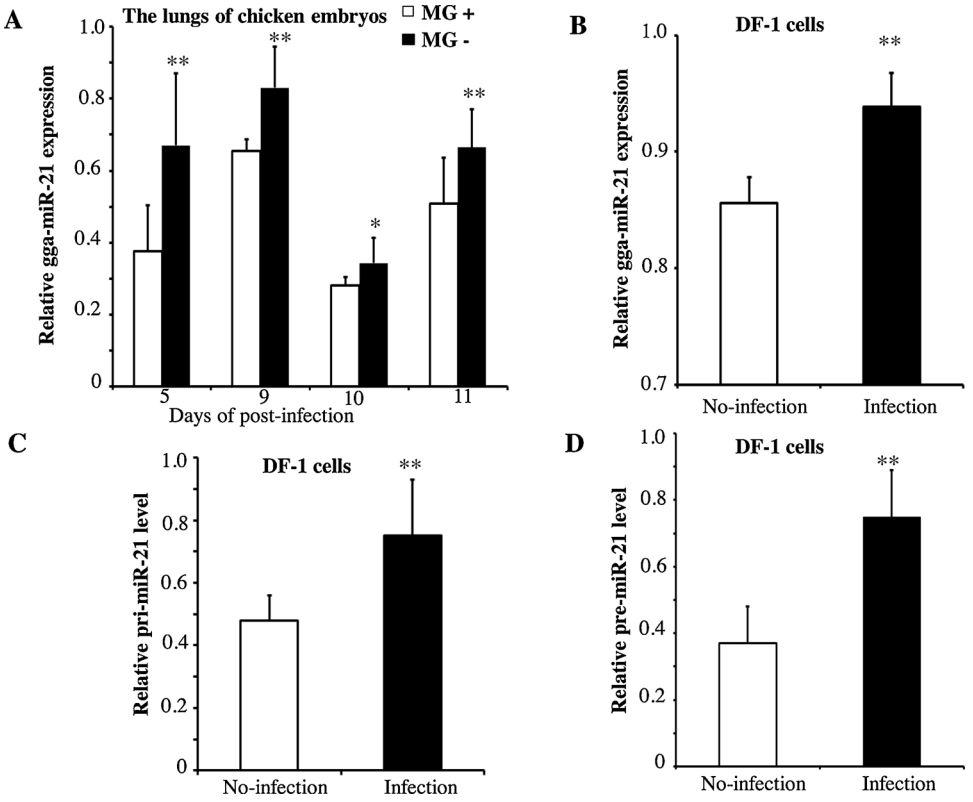

Fig. 1. gga-miR-21 expression is upregulated after MG infection. The chicken embryos were infected by MG-HS as described in Material and Methods. On the 5, 9, 10 and 11th days post-infection, the lungs of infected chicken embryos were processed, and the expression of gga-miR-21 was measured by RT-qPCR **(A)**. DF-1 cells were infected with MG-HS for 48 h, the levels of gga-miR-21 **(B)**, pri-miR-21 **(C)** and pre-miR-21 **(D)** were detected with RT-qPCR. All data are representative of at least three independent experiments ($^{*}P < 0.05$, $^{**}P < 0.01$).

3.5. MAP3K1 knockdown increases inflammatory cytokine production

To determine whether the observed effects of gga-miR-21 on inflammatory cytokine production in response to MG infection were, at least partially, mediated through

MAP3K1, we assessed the effects of silencing *MAP3K1* expression by siRNA and over-expressing *MAP3K1* expression by pcDNA3.1 vector on inflammatory cytokine production. DF-1 cells were transfected with siRNA-MAP3K1 (denoted as si-MAP3K1), a nonspecific control siRNA (denoted as siRNA-NC), pcDNA3.1-*MAP3K1* (denoted as pc-MAP3K1) or control pcDNA3.1, respectively. First, we confirmed that the siRNA significantly inhibited *MAP3K1* mRNA and protein expression in DF-1 cells (Fig. 5A), and pc-MAP3K1 substantially increased *MAP3K1* expression (Fig. 5C). ELISA revealed that knockdown of *MAP3K1* significantly up-regulated the protein levels of TNF-α, IL-1β, IL6, and IL8 in DF-1 cells (Fig. 5B). In contrast, the over-expression of endogenous *MAP3K1* significantly decreased the protein levels of TNF-α, IL-1β, IL6, and IL8 (Fig. 5D). Thus, these data strongly indicate that *MAP3K1* knockdown increases the production of inflammatory cytokines in DF-1 cells.

3.6. MAP3K1 knockdown activates NF-κB signaling via targeting MAP3K1

The results suggest that gga-miR-21 regulates MG-induced inflammatory cytokine expression by targeting *MAP3K1*. The findings of many recent studies support the theory that translocation of NF-κB p65 from the cytoplasm to the nucleus is a pivotal determinant of NF-κB activation (Mediero et al., 2014). To explore whether *MAP3K1* silencing intersects with the NF-κB signaling pathway, the NF-κB p65 expression was analyzed by an immunofluorescence assay. DF-1 cells in which *MAP3K1* was silenced by si-MAP3K1 or those treated with gga-miR-21 mimics showed that p65 (red) expression both increased upon deleting *MAP3K1* than those transfected with siRNA-NC or miR-21-NC (Fig. 6). The results suggest that gga-miR-21 activates NF-κB signaling via targeting *MAP3K1*.

3.7. gga-miR-21 inhibits MG propagation in DF-1 cells

To test whether gga-miR-21 has a biological function in MG propagation, DF-1 cells were transfected with gga-miR-21 mimic or miR-21-NC, followed by MG-HS infection. No-infection was used as another control group. Cells were harvested at 48 h post-infection, and the adhesion protein from MG-HS strain, namely pMGA1.2, was determined by RT-qPCR. The result showed that overexpression of gga-miR-21 significantly inhibited pMGA1.2 expression in DF-1 cells (Fig. 7), indicating that gga-miR-21 acts as a negative regulator of MG propagation in DF-1 cells.

3.8. gga-miR-21 promotes the Proliferation of the MG-Infected DF-1 Cells by Affecting the Cell cycle and Cell apoptosis

To further illuminate the biological significance of gga-miR-21 in MG-HS pathogenicity, gga-miR-21, miR-21-NC, miR-21-Inh or miR-21-Inh-NC were transfected into DF-1 cells, and then the cells co-cultured with MG-HS (8 μl at 10^{10} CCU/ml) for 42 h, In addition, the infected with MG-HS [denoted as miR-free (MG+)], and the no-infected DF-1cells [denoted as blank (MG-)] were used as a control groups. The cell growth assay, using real time cell analyzer system (RTCA), showed that the cell viability was decreased in all MG-infected groups [over-expression of gga-miR-21 (green), miR-21-NC (purple), miR-21-Inh (pink) or miR-21-Inh-NC (wathet) and miR-free (mazarine)] after MG infection compared to the blank MG- group (red), gga-miR-21 (green) remarkable increased the proliferation of DF-1 cells compared with miR-21-NC (purple) and the miR-free control (mazarine) (Fig. 8). Furthermore, miR-21-Inh (pink) remarkable decreased the proliferation of DF-1 cells after MG-HS infection, compared to the miR-21-Inh-NC (MG+) group (wathet) or the miR-free (MG+) group (mazarine) (Fig. 8). These results manifest that gga-miR-21 promotes DF-1 cell proliferation in MG-HS infection.

To further explore how gga-miR-21 promotes DF-1 cells proliferation, we detected the effect of gga-miR-21 on the cell cycle distribution

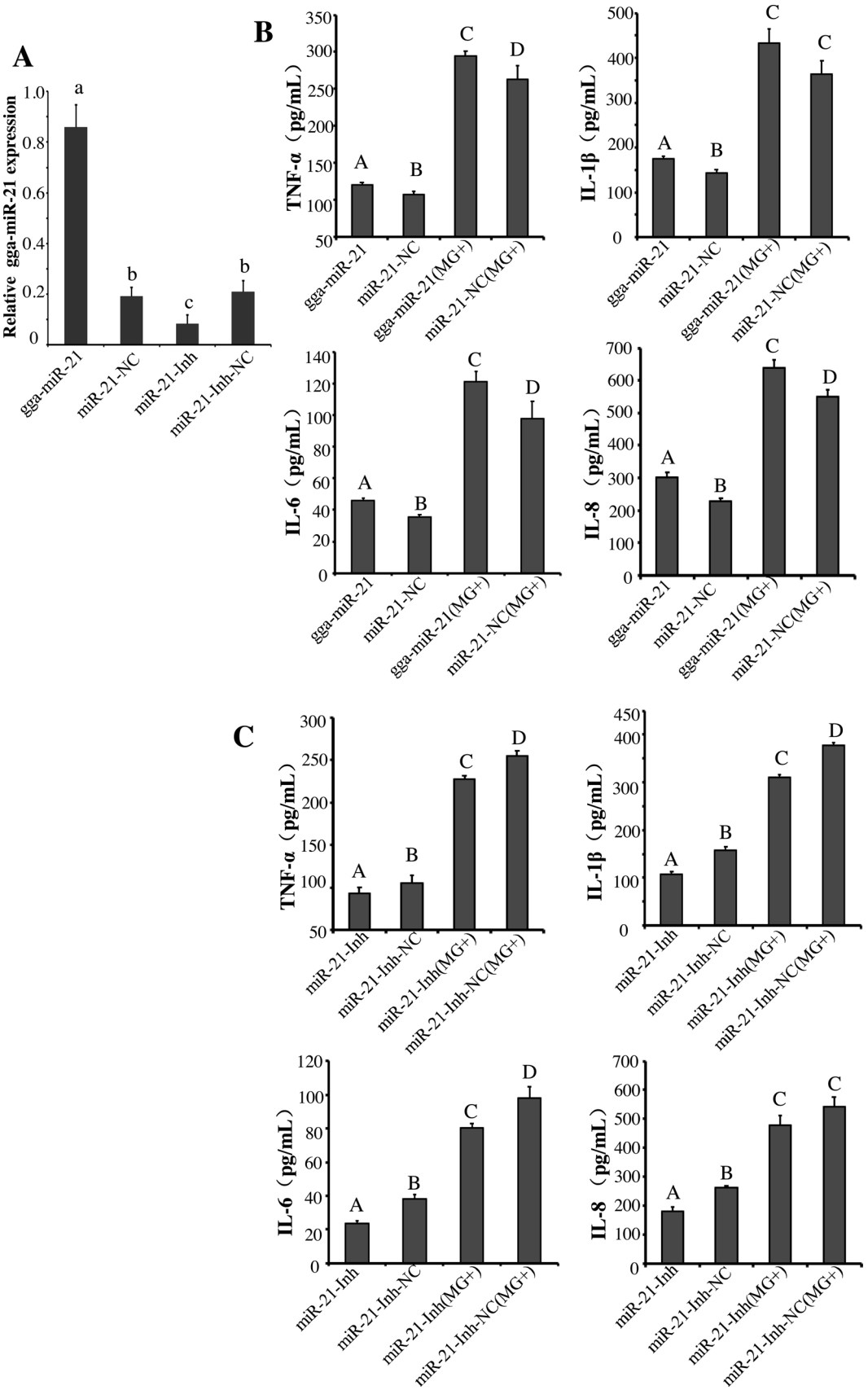

Fig. 2. gga-miR-21 induces MG-mediated production of inflammatory cytokines. **(A)** Over-expression of gga-miR-21 in DF-1 cells and transfection of miR-21-Inh reduced the expression of gga-miR-21 in DF-1 cells. **(B and C)** DF-1 cells were transfected with gga-miR-21, miR-21-NC, miR-21-Inh or miR-21-Inh-NC and were incubated for 24 h and then either left uninfected or infected with 130 μl of MG-HS for 36 h. The protein levels of TNF-α, IL-1β, IL6, and IL-8 were analyzed by ELISA at 36 h post-infection. Three independent experiments, each with three replicates, were performed. The data are presented as the means ± SEM. One-way ANOVA was used to analyze significant differences (Different capital letters represent $P < 0.05$, Different lowercase letters represent $P < 0.01$).

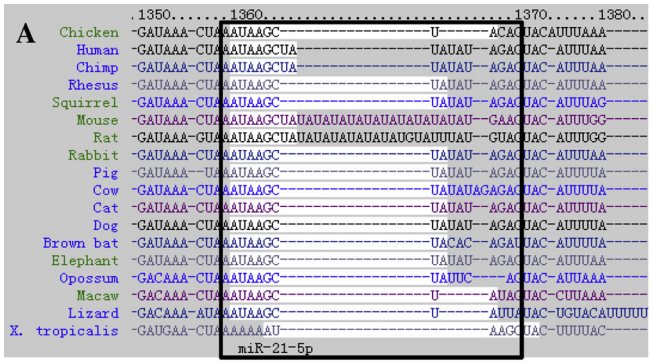

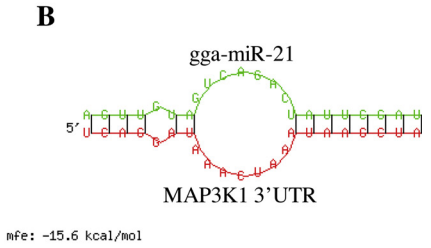

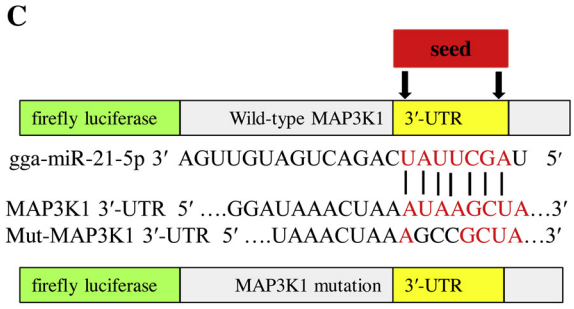

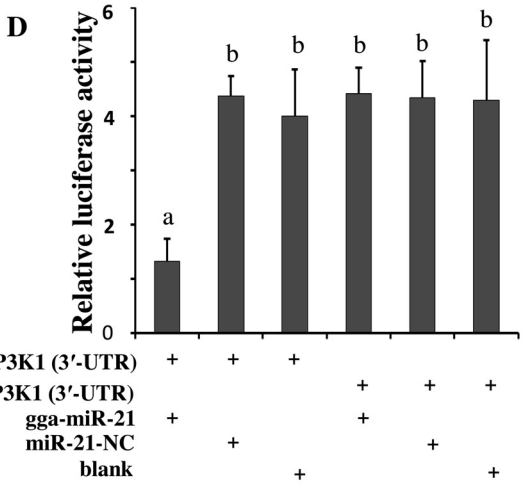

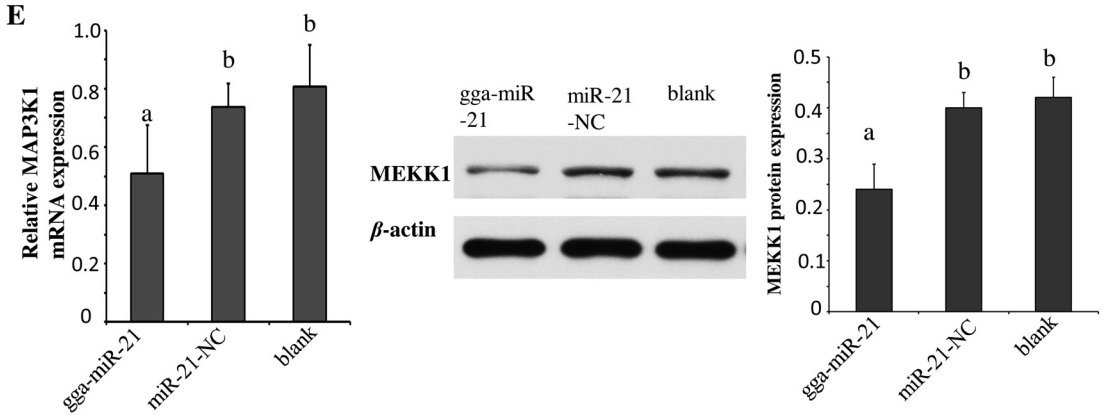

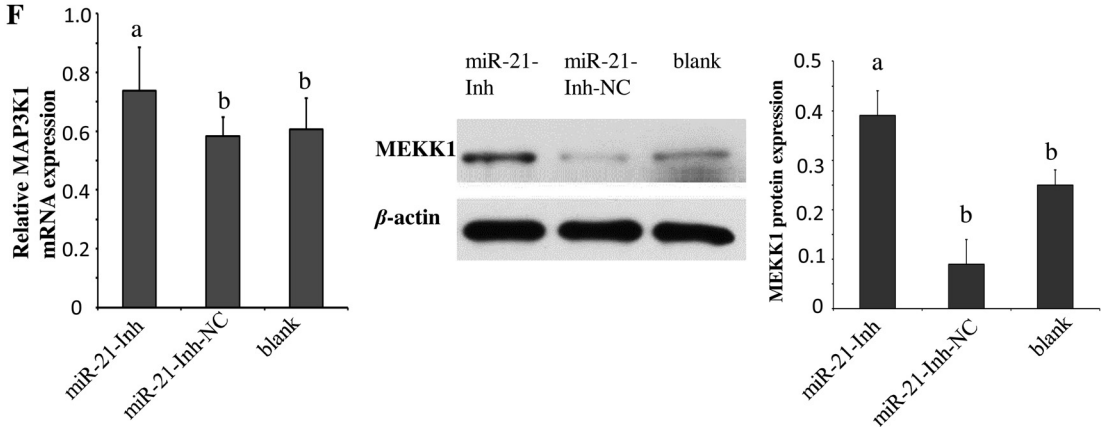

(caption on next page)

Fig. 3. gga-miR-21 directly targets to *MAP3K1*. **(A)** Sequence alignment of *MAP3K1* 3′-UTR from different species. The conserved target sequences are highlighted; **(B)** The predicted secondary structure of the RNA duplex of gga-miR-21 and *MAP3K1* 3′-UTR target site (Red: Target sequence; Green: gga-miR21); **(C)** psiCHECK-2 dual-luciferase reporter vector containing the 3′-UTR (wild-type or mutant) of *MAP3K1*. **(D)** DF-1 cells were co-transfected with Luc-MAP3K1 3′-UTR (wild-type or mutant) and the indicated RNA oligonucleotides. At 48 h post-transfection, the cells were assayed for both firefly and renilla luciferase activity through a dual-luciferase glow assay. **(E and F)** DF-1 cells were transfected with the indicated RNA oligonucleotides. At 48 h post-transfection, RT-qPCR detected the expression of the mRNA level of *MAP3K1*, Western blot analysis of MAP3K1 protein (MEKK1) expression. Three independent experiments, each with three replicates, were performed. The data are expressed as the means ± SDs. One-way ANOVA was used to analyze the significant differences (Different lowercase letters represent $P < 0.01$) (For interpretation of the references to colour in this figure legend, the reader is referred to the web version of this article.).

and cell apoptosis by flow cytometry. As above, DF-1 cells were transfected with the synthetic RNA oligonucleotides and then co-cultured with MG-HS (130 μl at 10^{10} CCU/ml) for 24 h. We demonstrated that MG-HS infection restrained mitosis by arresting the G1 cell cycle in the DF-1 cells, and that overexpression of gga-miR-21 generated cell cycle changes with a smaller proportion of cells in the G1-phase and a larger proportion of cells in the S- and G2-phases compared with miR-21-NC and the miR-free control. Nevertheless, gga-miR-21-Inh exerted contrasting effects and inhibited the cell cycle progression at the G1 phase more than miR-21-Inh-NC and the miR-free control **(**Fig. 9**)**. Cell apoptosis assay showed that gga-miR-21 has a key role in reducing apoptosis of DF-1 cells. The percentage of apoptotic DF-1 cells decreased when gga-miR-21 was overexpressed compared with miR-21-NC and the miR-free control, the opposite results were observed when gga-miR-21 was silenced **(**Fig. 10**)**. Collectively, these results show that gga-miR-21 suppresses MG propagation, and facilitates the proliferation of DF-1 cells by increasing the cell cycle progression and suppressing cell apoptosis.

4. Discussion

Innate immunity constitutes an essential immune defense against infection by microbial pathogens. Inflammation is characterized by marked production and release of inflammatory cytokines in immune reactions. *Mycoplasma* triggers rock-ribbed inflammation in organisms and produces a series of pro-inflammatory cytokines in many different cell types (Barton and Medzhitov, 2003). Emerging studies indicate that MG infection differentially regulates the expression of cellular miRNAs in chickens (Zhao et al., 2017). Multiple aberrant miRNAs can regulate host innate immune signaling pathways and mediate inflammatory responses. However, the role of miRNAs in MG-induced respiratory inflammation is largely unknown. Thus, in this study, we aimed to address the role of miRNA-regulated pathways in the MG-induced inflammation model.

miR-21 has appeared as a major miRNA both highly expressed and dynamically regulated in all kinds of cell types (Sheedy, 2015). It has been shown as a key switch involved in various models of airway inflammation (Moschos et al., 2007). However, the protective activity of miR-21 involving in MG-induced inflammation remains poorly understood. In our previous deep sequencing results, the up-regulation of gga-miR-21 was in lungs of MG-infected SPF chicken embryos was observed. In line with these results, this research discovered that the expression of gga-miR-21 was significantly up-regulated in the chicken embryonic lungs on the 5, 9, 10 and 11th days post-infection and the MG-infected DF-1 cells, whereas MAP3K1 had the opposite expression pattern. Moreover, we demonstrated that the overexpression of gga-miR-21 promoted the production of inflammatory cytokines (e.g., TNF-α, IL-1β, IL-6, and IL-8) by targeting *MA*P3K1, and inhibition of gga-miR-21expression resulted in decreased production of inflammatory cytokines. Interestingly, knockdown of *MAP3K1* with siRNA operated the same effects on inflammatory cytokines levels as was observed following gga-miR-21 overexpression, whereas overexpression of *MAP3K1* inhibited inflammatory cytokine production in DF-1 cells. Also, our findings demonstrated that gga-miR-21 and si-MAP3K1 activated the translocation of NF-κB from the cytoplasm to the nucleus, which in turn led to increased activation of inflammatory cytokine genes. Taken together, these results indicate that MG-induced gga-miR-21 acts as a potent pro-inflammatory miRNA in DF-1 cells.

MAPKs have been reported are key mediators of innate immune responses to pathogenic microorganism invasion. Upon recognition of Pathogen Associated Molecular Patterns (PAMPs), MAPKs are activated to promote inflammatory cytokines production to defend against pathogenic microorganism infection (Park et al., 2017). Our deep sequencing data also showed that MAPK pathway may be a pivotal regulatory route in regulating the host response to MG infection (Zhao et al., 2017). *MAP3K1* is a crucial member of the MAPK family. In human acute respiratory distress syndrome, *MAP3K1* was associated with increased IL-1β, IL-6, IL-8, and TNF-α production (Morrell et al., 2017).Thus, we believe that MG regulates MAPKs pathway through up-regulation of gga-miR-21 and down-regulation of *MAP3K1*. A bioinformatics software Kyoto Encyclopedia of Genes and Genomes (KEGG) showed that *MAP3K1* could negatively regulate NF-κB signaling

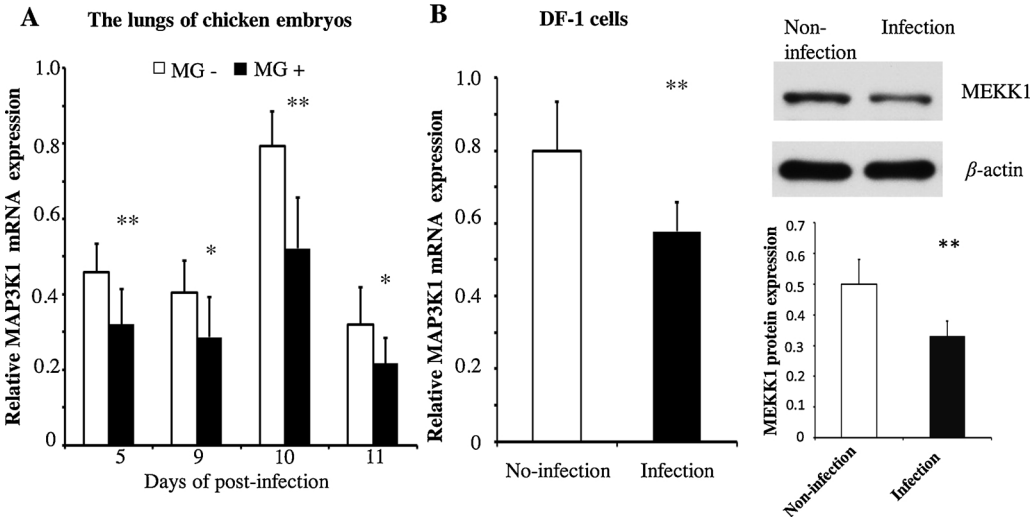

Fig. 4. MG infection downregulates the expression of *MAP3K1* in chicken embryo lungs (A) and DF-1 cells (B). Chicken embryos and DF-1 cells were infected with MG-HS as described in Materials and Methods, and the total RNA was extracted. *MAP3K1* mRNA expression was assessed by RT-qPCR normalized to GAPDH. MAP3K1 protein (MEKK1) expression was determined by Western blotting and normalized to β-actin. Three independent experiments, each with three replicates, were performed. The plotted data points show the means ± SDs, and the asterisks indicate statistically significant differences (*$P < 0.05$, **$P < 0.01$).

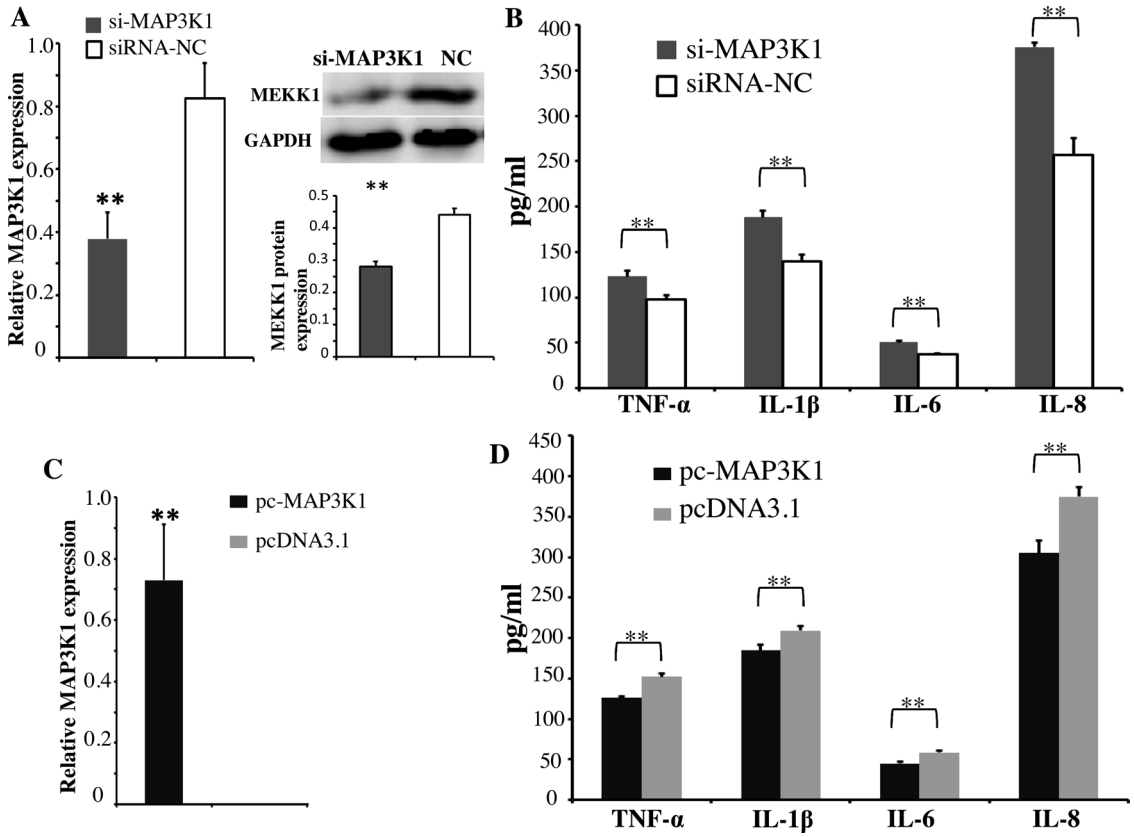

Fig. 5. *MAP3K1* knockdown increases inflammatory cytokine production. **(A)** DF-1 cells were transfected with si-MAP3K1 or siRNA-NC for 48 h. MAP3K1 mRNA levels and protein levels were measured by RT-qPCR and Western blotting, respectively. The expression of GAPDH was used as a loading control; **(C)** DF-1 cells were transfected with pc-MAP3K1 or pcDNA3.1 for 48 h. MAP3K1 mRNA expression was measured by RT-qPCR. The expression of GAPDH was used as a loading control; **(B and D)** The protein levels of TNF-α, IL-1β, IL6, and IL-8 were analyzed by ELISA at 48 h post-transfection. Three independent experiments, each with three replicates, were performed. The data are presented as the means ± SDs. Student's *t*-test was used to analyze significant differences$^{**}P < 0.01$.

pathway in chicken (https://www.kegg.jp/pathway/gga04010). In our previous studies, the MG-HS lipoproteins trigger-inflammatory responses via activation of the NF-κB signaling pathway were identified (Hu et al., 2016b). NF-κB promotes the production and release of inflammatory cytokines (e.g. IL-1β, IL-6, IL-8 and TNF-α) and plays a key role in the regulation of inflammatory responses (Toscano et al., 2011). miR-21 was identified as an immune system mediator and regulates the NF-κB signaling pathway by targeting immune-related genes, thus affecting microbial infection outcomes (Sheedy, 2015).These defense mechanisms were highly conserved, including regulation of cellular biological processes to defend against pathogenic microorganisms infection (Panayidou et al., 2014). It is reasonable to believe that gga-miR-21 plays a pivotal regulatory role in activating MAPKs and NF-κB pathways to regulate pro-inflammatory cytokines production by targeting *MAP3K1*.

The NF-κB mediated-immune response activated by miRNAs affects cell proliferation, cell apoptosis and microbial pathogen infections (Hu et al., 2016b; Yang and Wang, 2016). Such as, miR-181a/PTEN axis promotes colorectal cancer cell proliferation by activating NF-κB signaling pathway and then affect host anti-infection activity (Pei et al., 2016). In Marek's disease, overexpression of miR-221 and miR-222 decreased p27(Kip1) levels and inhibits the progression of T-cell lymphomas (Lambeth et al., 2009). miR-146a negatively regulated the activation of NF-κB signaling pathway and inhibited tumor cell migration and invasion by suppressing TRAF6 and IRAK1 (Taganov et al., 2006). Furthermore, pathogens infection modulates the cellular miRNA expression profile in animals, and the dysregulated miRNAs, in turn, affect the pathogen life cycle (Chang et al., 2014; Thirion and Ochiya, 2013). For example, miR-28, miR-125b, miR-198 and miR-223 restrain HIV replication via regulating host cellular factors or via targeting the HIV genome (Huang et al., 2007; Sung and Rice, 2009). miR-122 accelerates HCV replication by reinforcing its colony-forming ability (Masaki et al., 2015). gga-miR-21 inhibits the replication of infectious bursal disease virus through down-regulating the translation of VP1 gene in chicken fibroblasts (Wang et al., 2013). In the current research, we observed that gga-miR-21 negatively regulated MG propagation by inhibiting pMGA1.2 expression and promoted MG-infected cell proliferation, accelerated cycle progression and inhibited cell apoptosis. Together, the results reveal that gga-miR-21 inhibits MG propagation and improves cells proliferation by affecting cell cycle and apoptosis.

In summary, as illustrated in Fig. 11, these data indicated that the up-regulation of gga-miR-21 decreases *MAP3K1* expression in MG-infected tissues and cells, which in turn activates the MAPKs and NF-κB signaling pathways and promotes secretion of inflammatory cytokines to defend against MG infection. Furthermore, gga-miR-21 promotes the cell proliferation and cell cycle progression, and inhibits cell apoptosis. Therefore, targeting gga-miR-21 may provide a novel strategy for the diagnosis and treatment of mycoplasmosis. In addition, this study may also provide novel insight into the use of miRNA-based therapeutics against other inflammation-related diseases.

Authors' contributions

YZ, collection, assembly, and analysis of the data, manuscript writing, and data analysis; MZ, discussion and manuscript revision; YS and KZ, data analysis; XP, design, manuscript editing and revision. All authors read and approved the final manuscript for publication.

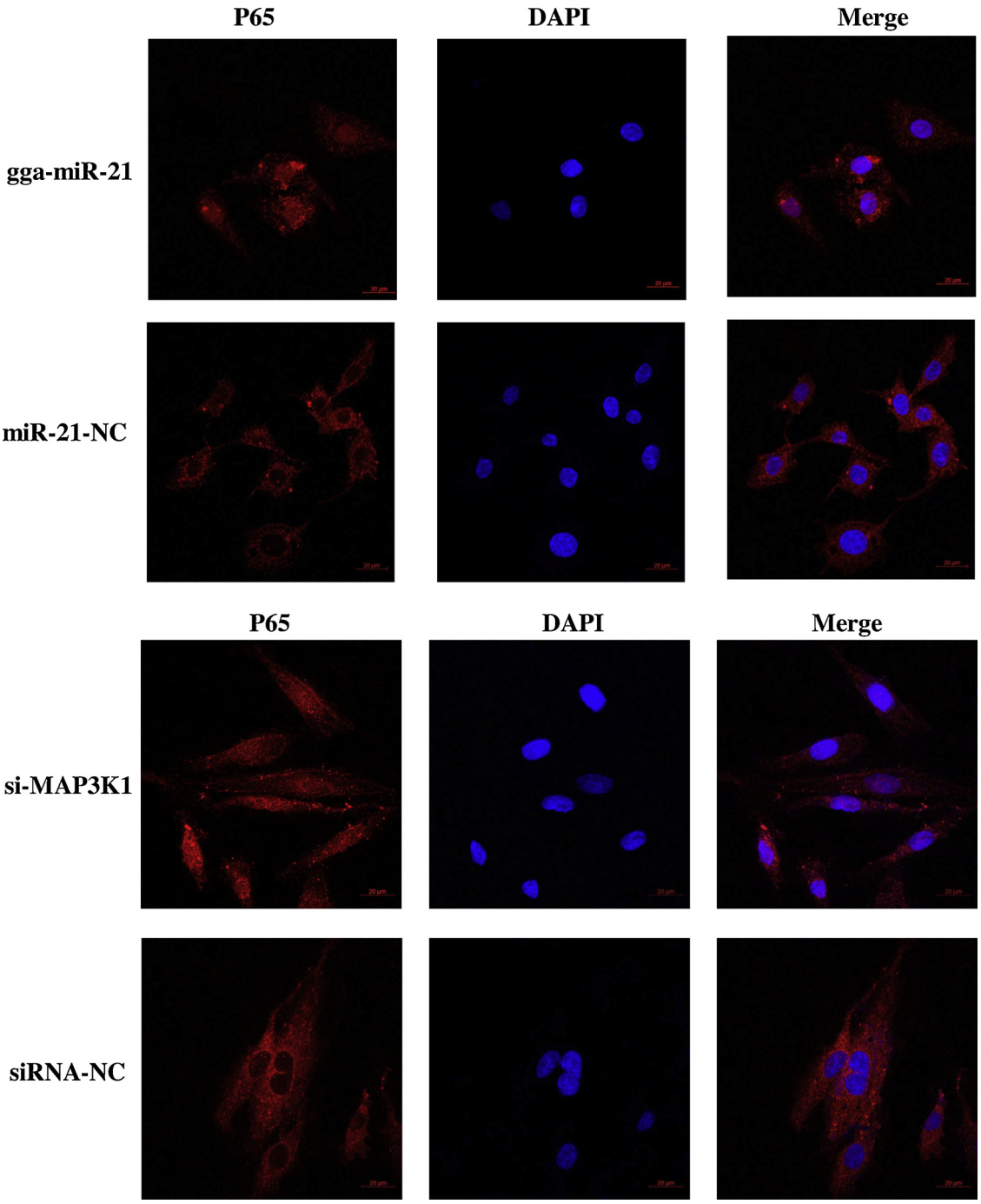

Fig. 6. NF-κB is activated following gga-miR-21 or si-MAP3K1. DF-1 cells were transfected with gga-miR-21or miR-21-NC **(A)**, si-MAP3K1 or siRNA-NC **(B)**, respectively. Nuclei were counterstained with 1 μg/mL DAPI, and NF-κB p65 (red) nuclear translocation was observed using a laser-scanning confocal microscope (For interpretation of the references to colour in this figure legend, the reader is referred to the web version of this article.).

Ethics approval and consent to participate

Our experimental protocols for chicken-embryo treatment were approved by the Institutional Animal Care and Use Committee of Huazhong Agricultural University. The procedures were carried out in accordance with the approved guidelines.

Consent for publication

Not applicable.

Availability of data and materials

All data generated or analyzed during this study are included in this published article.

Funding

This study was funded by the National Natural Science Foundation of China (Grant No.31972681) and the Fundamental Research Funds for the Central Universities (No. 2662017PY080).

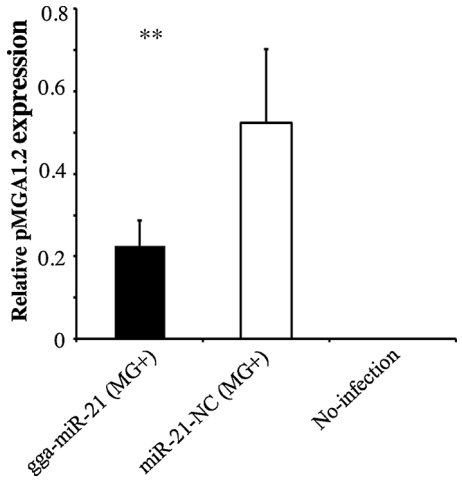

Fig. 7. gga-miR-21 downregulates MG propagation in DF-1 cells. DF-1 cells were transfected with gga-miR-21or miR-21-NC for 24 h and then infected with MG-HS. The cells were harvested at 48 h post-infection. pMGA1.2 mRNA level was determined by RT-qPCR and normalized to GAPDH. Three independent experiments, each with three replicates, were performed. The data are presented as the means ± SDs. One-way ANOVA was used to analyze significant differences$^{**}P < 0.01$.

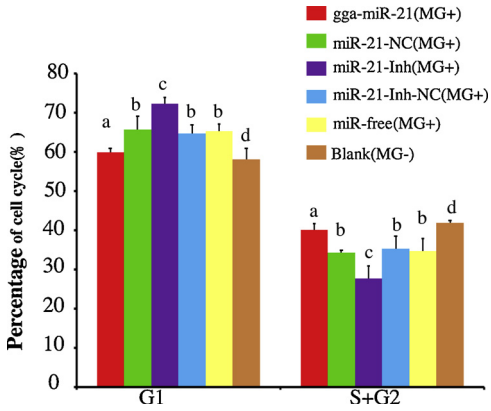

Fig. 9. The effect of the gga-miR-21 on the distribution of DF-1 cells in the cell cycle. DF-1 cells were transfected with gga-miR-21, miR-21-NC, miR-21-Inh or miR-21-Inh-NC and were incubated for 24 h. The cells then were infected with MG-HS strain. Four control groups, including miR-21-NC (MG+), miR-21-Inh-NC (MG+), miR-free (MG+) and blank (MG−) were used. At 24 h post-infection, the cell phase distribution was analyzed using a flow cytometer. Three independent experiments, each with three replicates, were performed. The data are presented as the means ± SDs. One-way ANOVA was used to analyze significant differences (Different lowercase letters represent $P < 0.01$ in G1 and S + G2 phase, respectively).

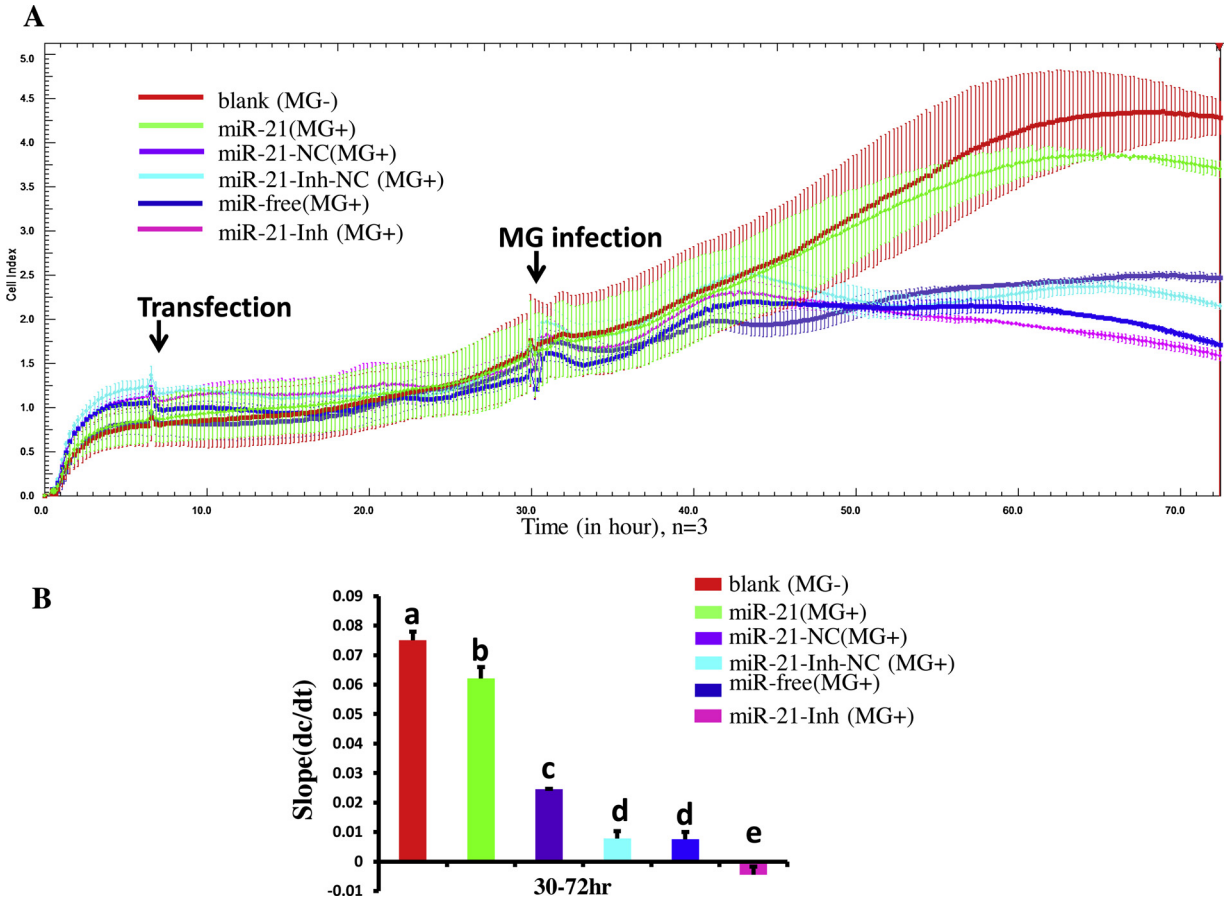

Fig. 8. The effect of gga-miR-21 on DF-1 cells proliferation. Real-time cell analyzer system (RTCA) was used to detect cell proliferation. DF-1 cells were transfected with gga-miR-21, miR-21-NC, miR-21-Inh or miR-21-Inh-NC and were incubated for 24 h. The cells were then infected with the MG-HS strain. Four control groups, including miR-21-NC (MG+), miR-21-Inh-NC (MG+), miR-free (MG+) and the blank (MG−), were used. **(B)** The analysis of slope of the lines in 42 h post-infection for **(A)**. Three independent experiments were performed in triplicate. The data are presented as the means ± SDs. One-way ANOVA was used to analyze significant differences (Different lowercase letters represent $P < 0.01$).

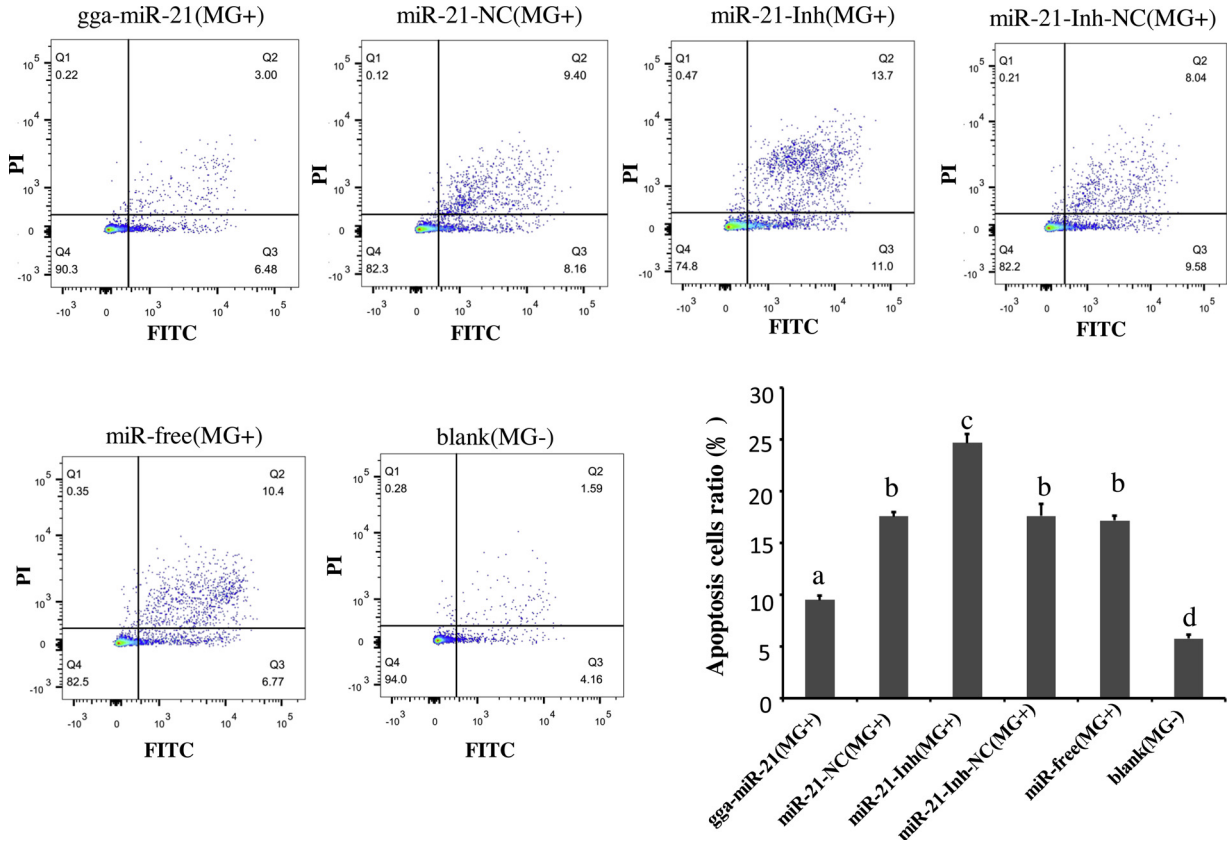

Fig. 10. gga-miR-21 inhibits DF-1 apoptosis in MG-HS infection. DF-1 cells were transfected with gga-miR-21, miR-21-NC, miR-21-Inh or miR-21-Inh-NC and were incubated for 24 h. The cells then were infected with MG-HS strain, harvested and stained with anti-annexin V-propidium iodide, and analyzed by flow cytometer after 24 h post-infection. Four control groups, including miR-21-NC (MG+), miR-21-Inh-NC (MG+), miR-free (MG+) and blank (MG−), were used. Three independent experiments, each with three replicates, were performed. The data are presented as the means ± SDs. One-way ANOVA was used to analyze significant differences (Different lowercase letters represent $P < 0.01$).

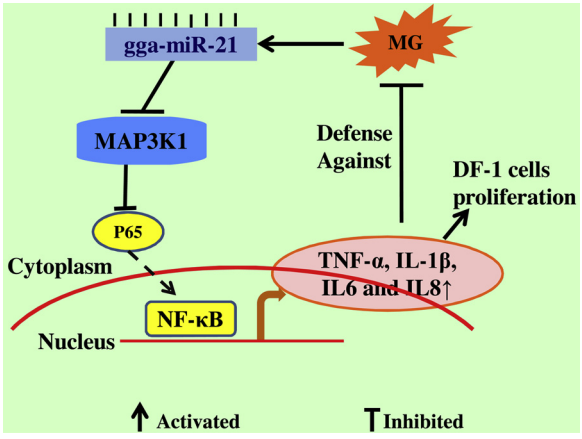

Fig. 11. A graphic abstract showing the major findings of this study. Schematic diagram of the gga-miR-21/ MAP3K1/ NF-κB pathway in DF-1 cells and its roles in defense against MG infection. gga-miR-21 regulated DF-1 cells proliferation by affecting the cell cycle and cell apoptosis.

Declaration of Competing Interest

The authors declare that they have no competing interests.

Acknowledgment

The authors are grateful to Yanzhang Gong, Yanping Feng, Shijun Li and Zheya Sheng for their suggestions to this paper.

References

Ambros, V., 2004. The functions of animal microRNAs. Nature 431, 350.
Barton, G.M., Medzhitov, R., 2003. Toll-like receptor signaling pathways. Science 300, 1524.
Bazzoni, F., Rossato, M., Fabbri, M., Gaudiosi, D., Mirolo, M., Mori, L., Tamassia, N., Mantovani, A., Cassatella, M.A., Locati, M., 2009. Induction and regulatory function of miR-9 in human monocytes and neutrophils exposed to proinflammatory signals. Proc. Natl. Acad. Sci. U.S.A. 106, 5282–5287.
Bi, D., Ji, X., 1988. The Isolation and Identification of the Mycoplasma Gallisepticum. Acta Veterinaria et Zootechnica Sinica 1.
Bi, D., Xu, Q., 1997. Study on pathogenicity of HS strain Mycoplasma gallisepticum. Chin. J. Animal and Poultry Infections Dis. 24–26.
Chang, H.L., Ji, H.K., Lee, S.W., 2014. The role of microRNAs in Hepatitis C Virus replication and related liver diseases. J. Microbiol. 52, 445–451.
Chen, J., Wang, Z., Bi, D., Hou, Y., Zhao, Y., Sun, J., Peng, X., 2015. Gga-miR-101-3p plays a key role in Mycoplasma gallisepticum (HS strain) infection of chicken. Int. J. Mol. Sci. 16, 28669–28682.
Cookson, K.C., Shivaprasad, H.L., 1994. Mycoplasma gallisepticum infection in chukar partridges, pheasants, and peafowl. Avian Dis. 38, 914–921.
Ferreromiliani, L., Nielsen, O.H., Andersen, P.S., Girardin, S.E., 2007. Chronic inflammation: importance of NOD2 and NALP3 in interleukin-1beta generation. Clin. Exp. Immunol. 147, 227.
Hayden, M.S., Ghosh, S., 2008. Shared principles in NF-κB signaling. Cell 132, 344–362.
Hu, F., Zhao, C., Bi, D., Tian, W., Chen, J., Sun, J., Peng, X., 2016a. Mycoplasma gallisepticum (HS strain) surface lipoprotein pMGA interacts with host apolipoprotein A-I during infection in chicken. Appl. Microbiol. Biotechnol. 100, 1343–1354.
Hu, Q., Zhao, Y., Wang, Z., Hou, Y., Bi, D., Sun, J., Peng, X., 2016b. Chicken gga-miR-19a targets ZMYND11 and plays an important role in host defense against Mycoplasma gallisepticum (HS strain) infection. Front. Cell. Infect. Microbiol. 6, 102.
Huang, J., Wang, F., Argyris, E., Chen, K., Liang, Z., Tian, H., Huang, W., Squires, K., Verlinghieri, G., Zhang, H., 2007. Cellular microRNAs contribute to HIV-1 latency in resting primary CD4+ T lymphocytes. Nat. Med. 13, 1241.
Hutchison, E.R., Kawamoto, E.M., Taub, D.D., Lal, A., Abdelmohsen, K., Zhang, Y., Iii, W.H.W., Lehrmann, E., Camandola, S., Becker, K.G., 2013. Evidence for miR-181 involvement in neuroinflammatory responses of astrocytes. Glia 61, 1018–1028.
Kim, H., Kataru, R.P., Koh, G.Y., 2014. Inflammation-associated lymphangiogenesis: a double-edged sword? J. Clin. Invest. 124, 936–942.

Lambeth, L.S., Yao, Y., Smith, L.P., Zhao, Y., Nair, V., 2009. MicroRNAs 221 and 222 target p27Kip1 in Marek's disease virus-transformed tumour cell line MSB-1. J. Gen. Virol. 90, 1164.
Livak, K.J., Schmittgen, T.D., 2001. Analysis of relative gene expression data using real-time quantitative PCR and the $2-\Delta\Delta CT$ method. Methods 25, 402–408.
Lu, T.X., Munitz, A., Rothenberg, M.E., 2009. MicroRNA-21 is up-regulated in allergic airway inflammation and regulates IL-12p35 expression. J. Immunol. 182, 4994.
Masaki, T., Arend, K.C., Li, Y., Yamane, D., Mcgivern, D.R., Kato, T., Wakita, T., Moorman, N.J., Lemon, S.M., 2015. miR-122 stimulates hepatitis C virus RNA synthesis by altering the balance of viral RNAs engaged in replication versus translation. Cell Host Microbe 17, 217.
Mediero, A., Perezaso, M., Cronstein, B.N., 2014. Activation of EPAC1/2 is essential for osteoclast formation by modulating NFκB nuclear translocation and actin cytoskeleton rearrangements. Faseb Journal Official Publication of the Federation of American Societies for Experimental Biology 28, 4901–4913.
Morrell, E.D., O'Mahony, D.S., Glavan, B.J., Harju-Baker, S., Nguyen, C., Gunderson, S., Abrahamson, A., Radella, I.F., Rona, G., Black, R.A., 2017. Genetic variation in MAP3K1 associates with ventilator-free days in acute respiratory distress syndrome. Am. J. Respir. Cell Mol. Biol.
Moschos, S.A., Williams, A.E., Perry, M.M., Birrell, M.A., Belvisi, M.G., Lindsay, M.A., 2007. Expression profilingin vivodemonstrates rapid changes in lung microRNA levels following lipopolysaccharide-induced inflammation but not in the anti-inflammatory action of glucocorticoids. BMC Genomics 8, 240.
Panayidou, S., Ioannidou, E., Apidianakis, Y., 2014. Human pathogenic bacteria, fungi, and viruses in Drosophila: disease modeling, lessons, and shortcomings. Virulence 5, 253–269.
Park, J.H., Lee, B., Kim, H.K., Kim, E.Y., Kim, J.H., Min, J.H., Kim, S., Sohn, Y., Jung, H.S., 2017. Peimine inhibits the production of proinflammatory cytokines through regulation of the phosphorylation of NF-κB and MAPKs in HMC-1 cells. Pharmacogn. Mag. 13, S359–S364.
Pei, H., Tan, F.B., Liu, L., Yu, N.H., Zhu, H.J.A., 2016. IL-1β/NF-kb signaling promotes colorectal cancer cell growth through miR-181a/PTEN axis. Arch. Biochem. Biophys. 604, 20–26.
Rodrigues, P.M., Afonso, M.B., Simão, A.L., Borralho, P.M., Rodrigues, C.M.P., Rui, E.C., 2016. Corrigendum: inhibition of NF-κB by deoxycholic acid induces miR-21/PDCD4-dependent hepatocellular apoptosis. Sci. Rep. 6, 27828.
Sheedy, F.J., 2015. Turning 21: induction of miR-21 as a key switch in the inflammatory response. Front. Immunol. 6.
Sung, T.L., Rice, A.P., 2009. miR-198 inhibits HIV-1 gene expression and replication in monocytes and its mechanism of action appears to involve repression of cyclin T1. PLoS Pathog. 5, e1000263.
Taganov, K.D., Boldin, M.P., Chang, K.J., Baltimore, D., 2006. NF-κB-Dependent induction of MicroRNA MiR-146, an inhibitor targeted to signaling proteins of innate immune responses. Proc. Natl. Acad. Sci. U.S.A. 103, 12481.
Thirion, M., Ochiya, T., 2013. Roles of microRNAs in the hepatitis B virus infection and related diseases. Viruses 5, 2690–2703.
Toscano, M.A., Campagna, L., Molinero, L.L., Cerliani, J.P., Croci, D.O., Ilarregui, J.M., Fuertes, M.B., Nojek, I.M., Fededa, J.P., Zwirner, N.W., 2011. Nuclear factor (NF)-κB controls expression of the immunoregulatory glycan-binding protein galectin-1. Mol. Immunol. 48, 1940–1949.
Wang, Y.S., Ouyang, W., Pan, Q.X., Wang, X.L., Xia, X.X., Bi, Z.W., Wang, Y.Q., Wang, X.M., 2013. Overexpression of microRNA gga-miR-21 in chicken fibroblasts suppresses replication of infectious bursal disease virus through inhibiting VP1 translation. Antiviral Res. 100, 196.
Winner, F., Rosengarten, R., Citti, C., 2000. In vitro cell invasion of Mycoplasma gallisepticum. Infect. Immun. 68, 4238–4244.
Yang, Y., Wang, J.K., 2016. The functional analysis of MicroRNAs involved in NF-κB signaling. Eur. Rev. Med. Pharmacol. Sci. 20, 1764.
Zhao, Y., Hou, Y., Zhang, K., Yuan, B., Peng, X., 2017. Identification of differentially expressed miRNAs through high-throughput sequencing in the chicken lung in response to Mycoplasma gallisepticum HS. Comparative biochemistry and physiology. Part D. Genomics & proteomics 22, 146–156.